Supplemental Figure 1

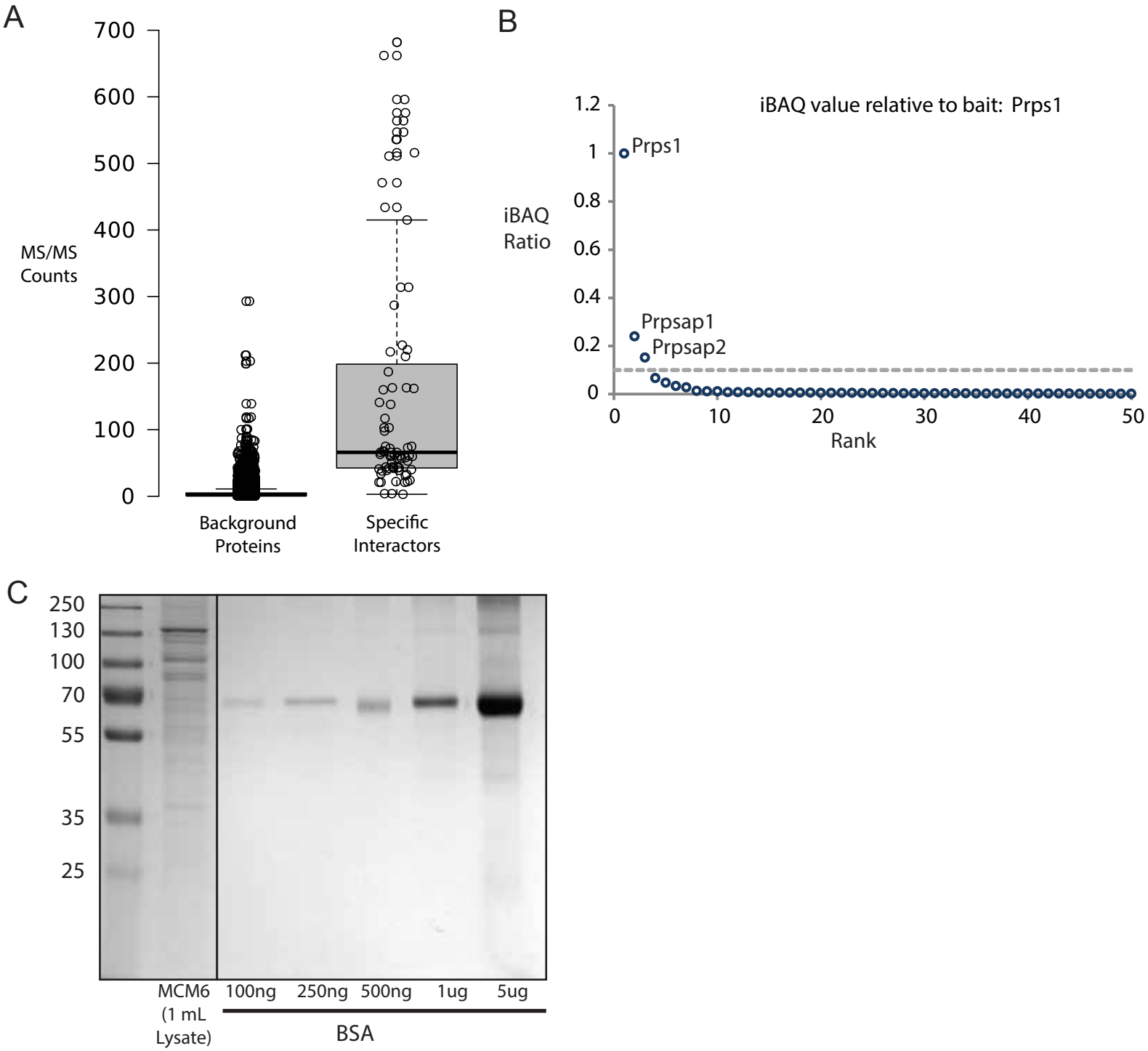

Supplemental Figure 1: High-stringency washes effectively and specifically purify bait-interacting proteins

A) Proteins identified as specific interactors by LFQ analysis show on average many more MS/MS spectral counts than background proteins. B) Representative calculation of iBAQ value relative to bait for Prps1 xIP-MS pulldown (after cross-linking). iBAQ values, calculated in MaxQuant, are a measure of protein abundance. The dashed grey line indicates an iBAQ ratio of 0.1 relative to Prps1. C) GFP-based affinity purification from crude whole cell lysates obtains approximately hunderds of nanograms of protein for cross-linking analysis.

Supplemental Figure 2

A

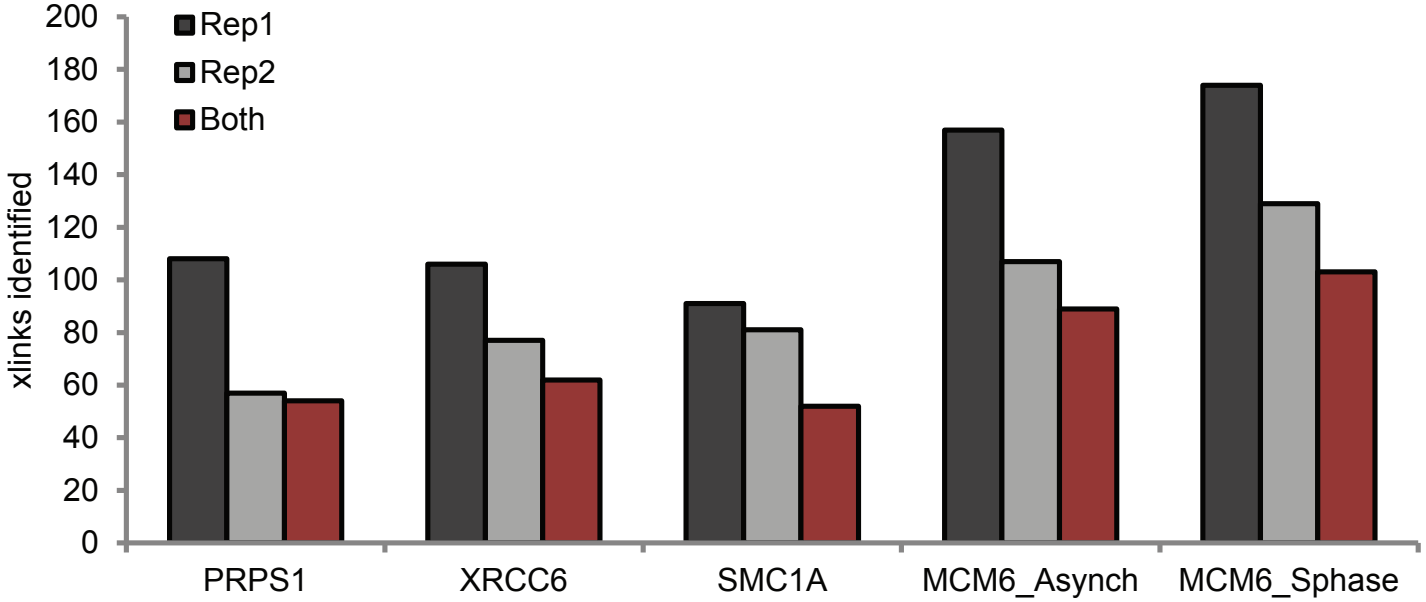

Supplemental Figure 2: xIP-MS identifies reproducible, high-confidence cross-links for chromatin-associated protein complexes

A) Duplicate xIP-MS experiments were performed for each protein complex analyzed in this study. Only cross-linked sites identified in both experiments with both peptides 5 >= length >= 40, indicated by the red column in the bar graph, were considered as high-confidence cross-linked sites for structural analysis.

Supplemental Figure 3

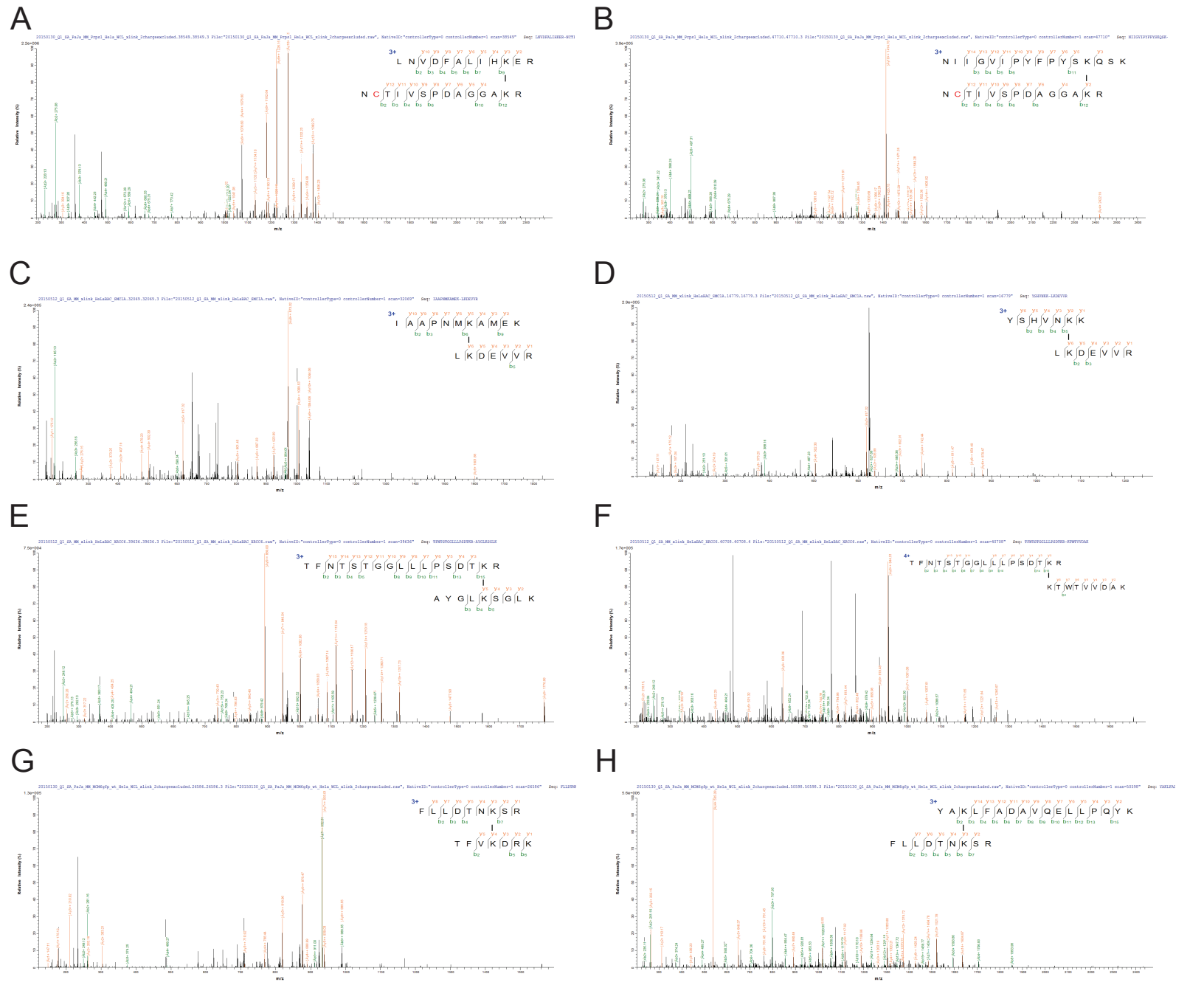

Supplemental Figure 3: Representative spectral matches from high-confidence cross-linked peptide identifications

A representative intra- and inter-protein spectral match from each bait is displayed. A) PRPS1-176:PRPS1-194 intra-link. B) PRPS1-176:PRPSAP1-103 inter-link. C) SMC1A-213:SMC1A-1026 intra-link. D) SMC1A-213:SMC3-984 inter-link. E) XRCC6-317:XRCC6-591 intra-link. F) XRCC6-317:XRCC6-274 inter-link. G) MCM6_Asynch-99:MCM6_Asynch-197 intra-link. H) MCM6_Asynch-197:MCM7_Asynch-75 inter-link.

Supplemental Figure 4

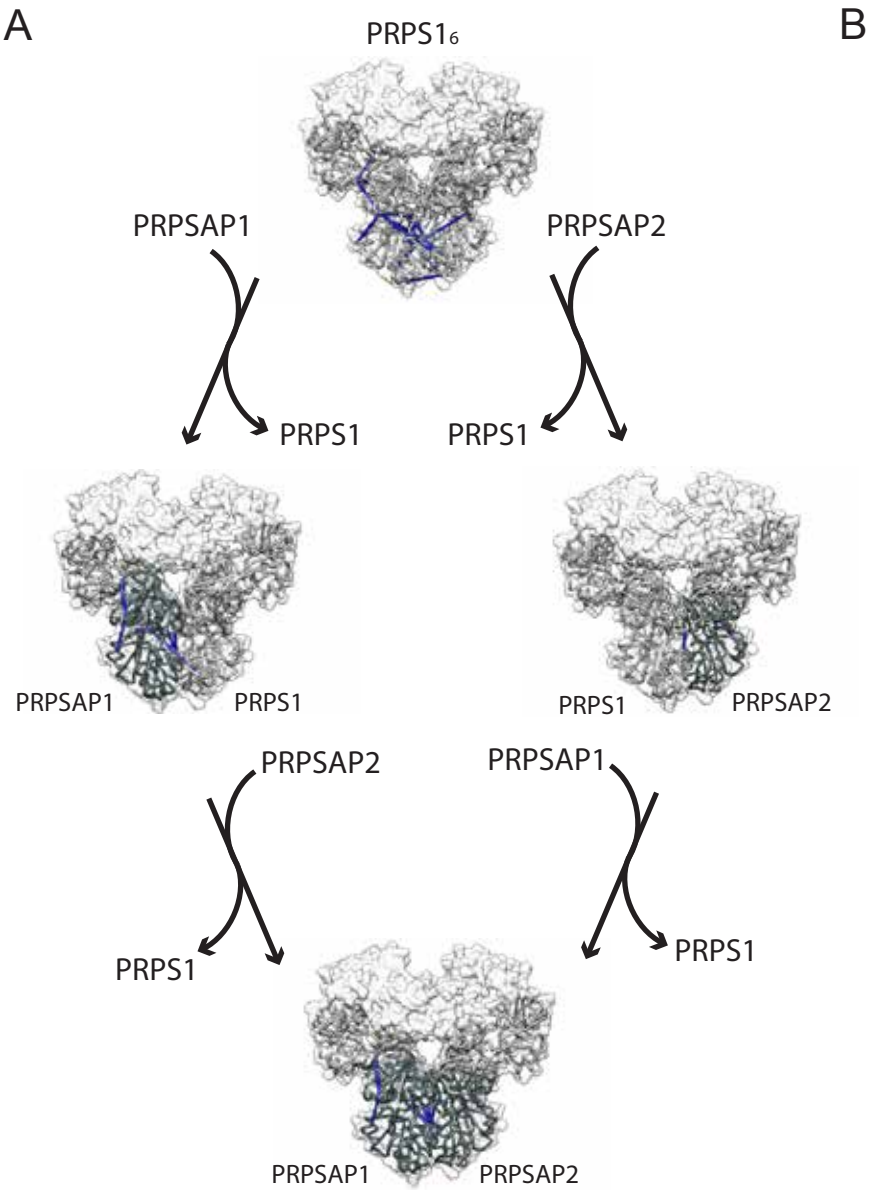

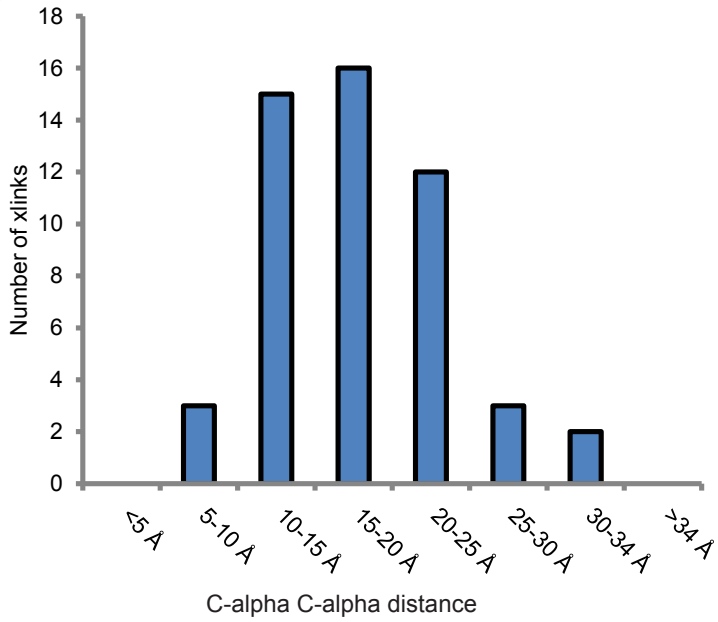

Supplemental Figure 4: A structural ensemble of PRPP complexes

A) Cross-linking evidence for PRPS1 subunit replacement by PRPSAP1 (PDB: 2c4k) and PRPSAP2 (PDB: 2ji4). Cross-links were mapped by directly fitting PRPSAP1 (RMSD: 0.901 Å with PRPS1) or PRPSAP2 (RMSD: 0.889 Å with PRPS1) over the respective PRPS1 subunit using MatchMaker in UCSF Chimera. PRPS1 subunits are colored in light grey, and PRPSAP1 or PRPSAP2 subunits are colored in dark grey as indicated. B) All mapped PRPP cross-link distances are displayed as a histogram. All 51 observed, unambiguous cross-links mapped onto this ensemble of structures within a 34 Å distance constraint.

Supplemental Figure 5

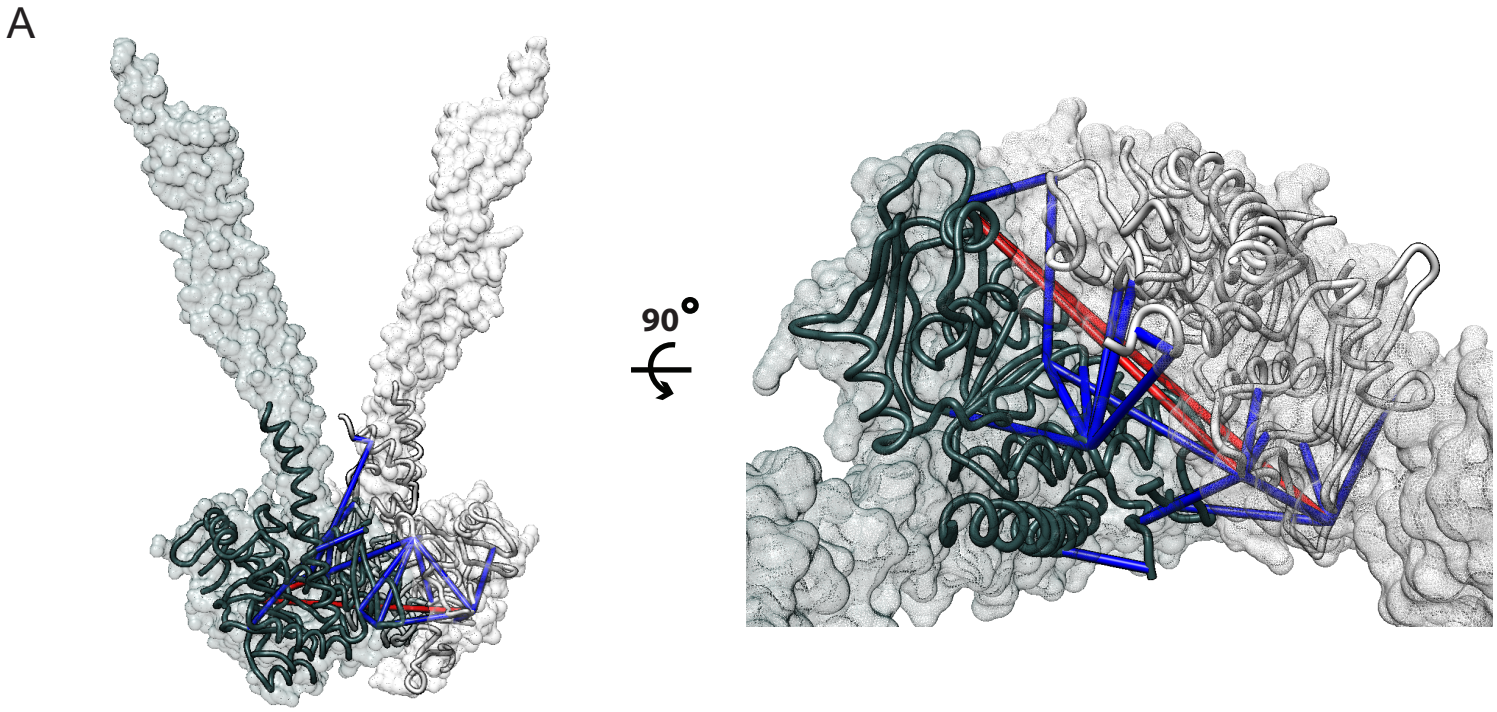

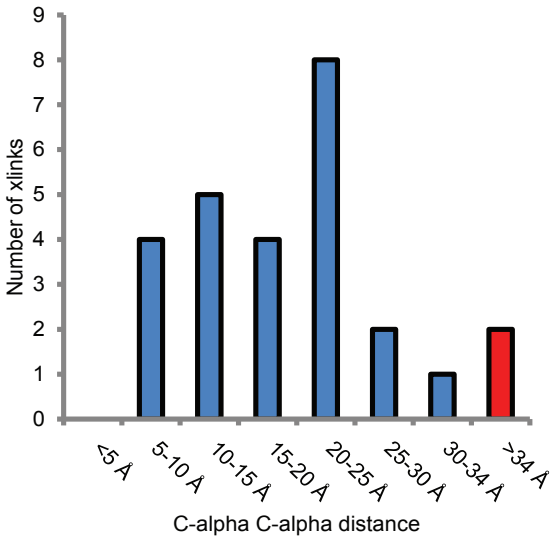

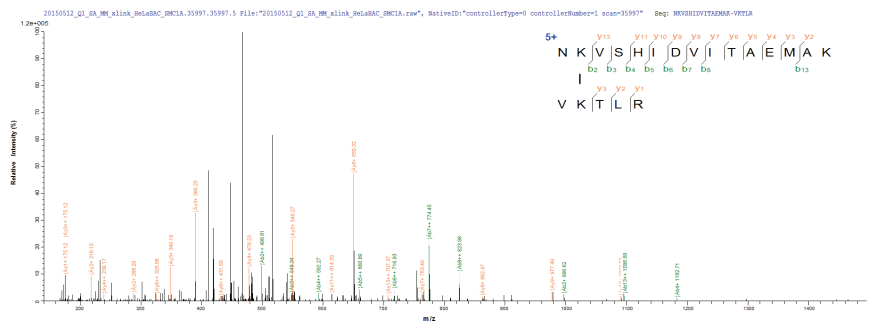

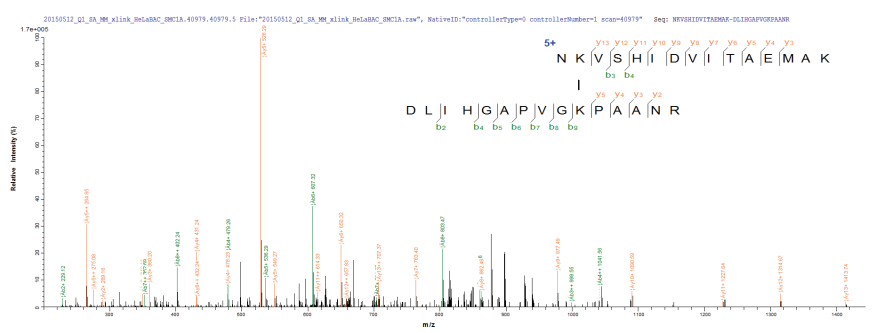

Supplemental Figure 5: A model for SMC1A/SMC3 head interactions

A) A homology based model for the SMC1A/SMC3 head interaction, with SMC1A in light grey and SMC3 in dark grey. The SMC3 dimer surface from the PDB: 4ux3 crystal structure used for aligning the SMC1A and SMC3 models is shown in silhouette. 24/26 cross-links map to this model within a distance constraint of 34 Å. The two violating cross-links lie on opposite sides of the head interface. B) The SMC1A model is colored in light grey, and the SMC3 model is colored in dark grey. Both were aligned with their mouse counterparts from PDB: 2wd5. Cross-links are displayed in blue. C) Histogram of combined cross-link distances from our SMC1A/SMC3 head and hinge domain models. Cross-links exceeding a constraint of 34 Å are colored in red, as in (A) and (B). D) Representative spectral match from SMC1A-72:SMC3-1194, a cross-link which exceeded 34 Å. E) Representative spectral match from SMC1A-59:SMC3-1194, a cross-link which exceeded 34 Å.

Supplemental Figure 6

A

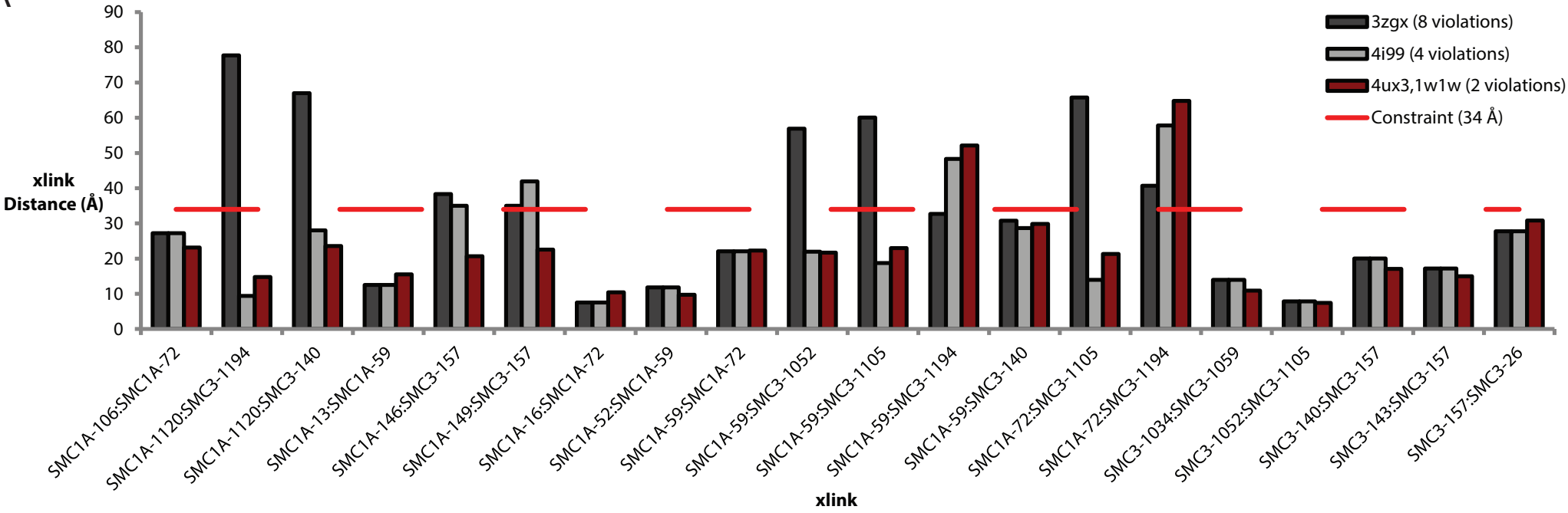

Supplemental Figure 6: Identified cross-links best fit homology models built from eukaryotic cohesin

A) We utilized a homology-based approach to model the heterodimeric SMC1A and SMC3 head domain interaction using prokaryote (PDB: 3zgx), archaea (PDB: 4i99) and eukaryote (PDB: 1w1w and PDB: 4ux3) dimeric SMC homologs. All cross-links mappable onto all three models are displayed with their respective distances. The eukaryote-based model exhibits the fewest violations, with both cross-link violations located between the heterodimeric interface.

Supplemental Figure 7

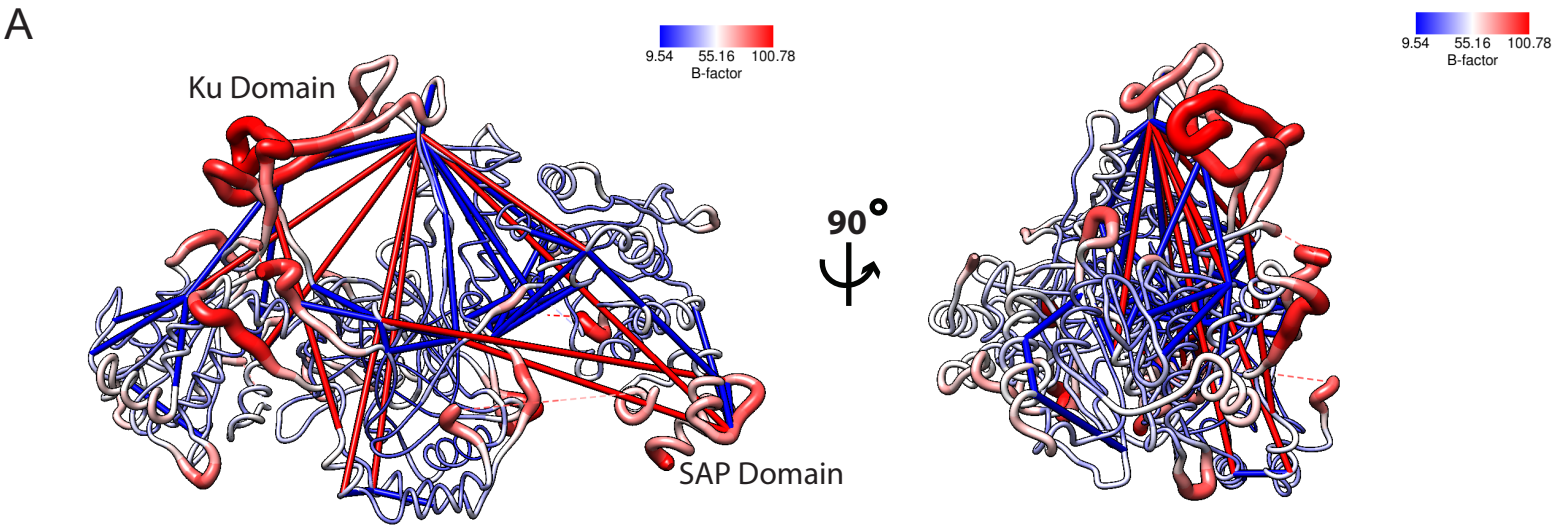

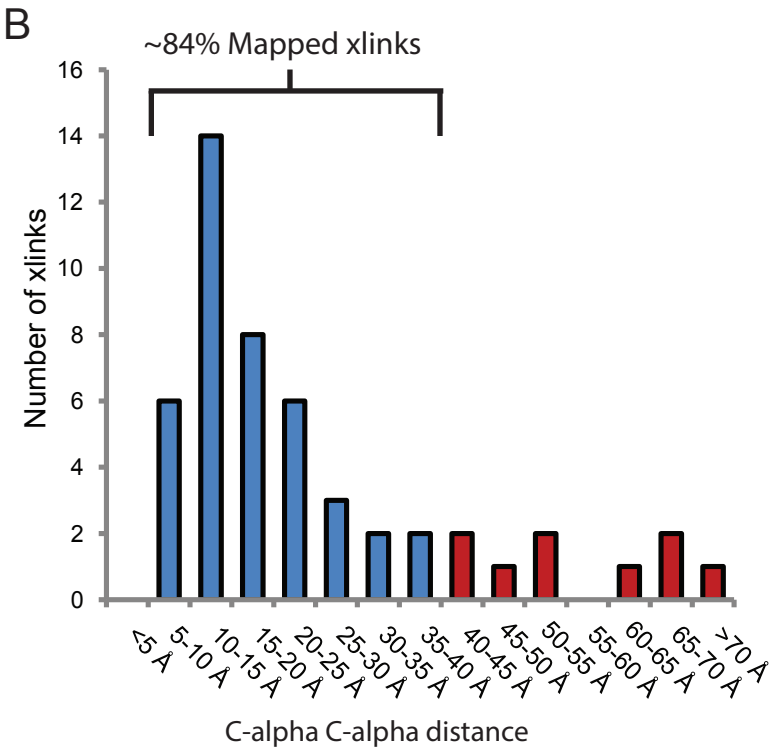

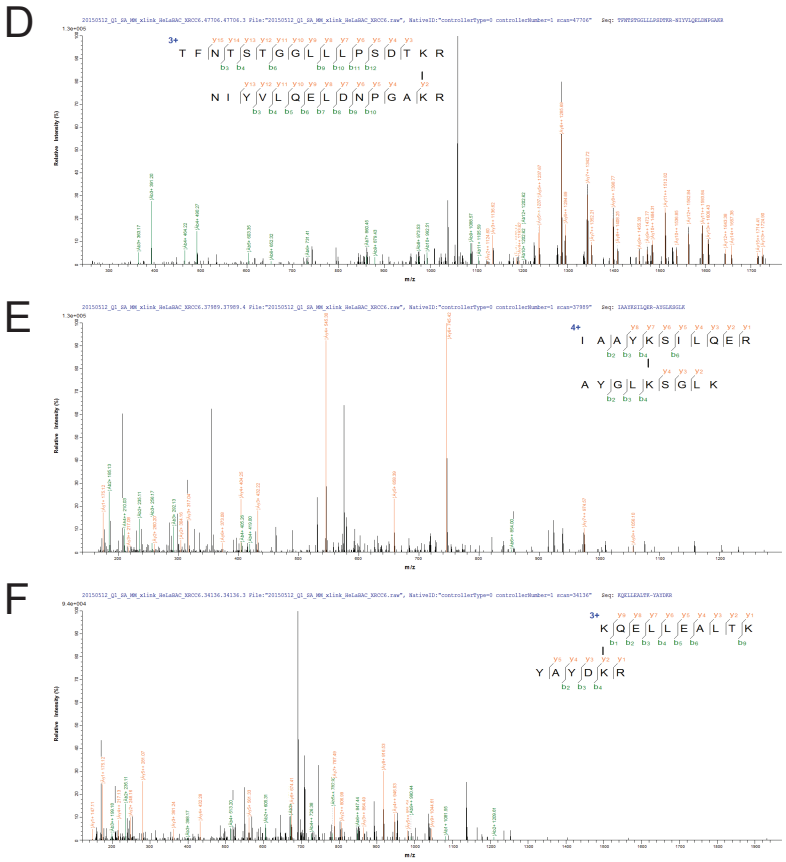

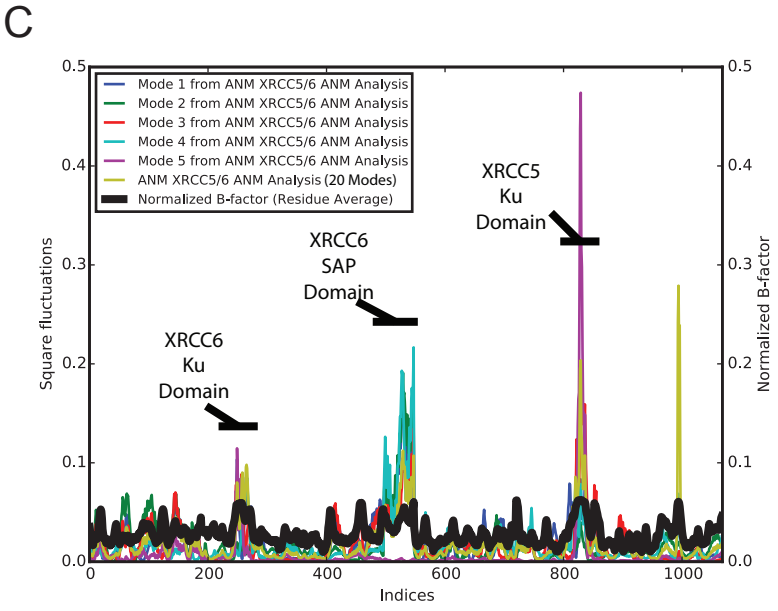

Supplemental Figure 7: xIP-MS reveals conformational flexibility in XRCC5/6

A) The XRCC5/6 with mapped cross-links is displayed as described in Figure 5. The complex is rotated around the vertical axis to make the passage of DNA through the Ku domain ring clear, as well as the proposed movement of the Ku domain in the vertical axis. The protein backbone is colored by residue average B-factor as indicated in the key, and the protein backbone radius is scaled similarly. B) Cross-link distances mapped onto XRCC5/6. Distances exceeding 40 Å, which we considered as indicating potential conformational shifts, are colored in red. C) Analysis of normal modes indicates conformational flexibility in the Ku and SAP domains of XRCC5/6. Normalized square fluctuations from the five slowest frequency modes (square of mode vector multiplied by variance), the normalized sum of square fluctuations for the twenty lowest frequency modes, and the normalized residue average B-factor are shown as indicated in the legend. D-F) Representative spectral matches from XRCC5/6 cross-link violations. D) XRCC6-114:XRCC6-317 intra-link. E) XRCC6-591:XRCC5-265 inter-link. F) XRCC6-596:XRCC5-399 inter-link.

Supplemental Figure 8

A

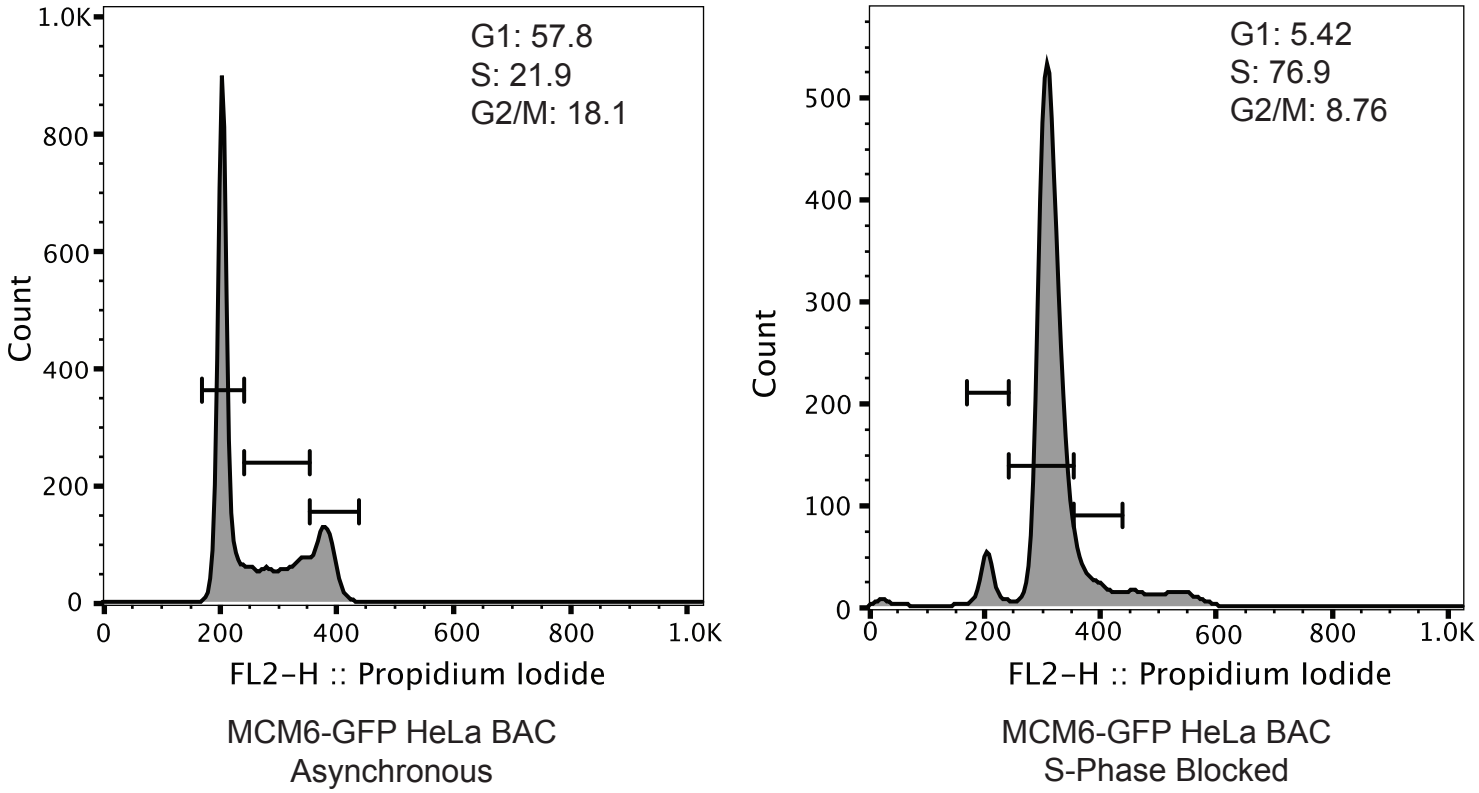

Supplemental Figure 8: FACS analysis of S-phase thymidine synchronization

A) Propidium iodide staining and FACS analysis confirmed synchronization in S-phase after overnight thymidine treatment.

Table 1: MaxQuant protein identifications and LFQ analysis
Table 2: pLink cross-linked peptide spectral matches at 0.05 FDR
Table 3: High confidence, filtered cross-linked sites identified by xIP-MS
Supplemental Video 1: Example normal modes from XRCC5/6 analysis